Structure–activity relationships of trimethoxybenzyl piperazine N-type calcium channel inhibitors

Hassan Pajouhesh [a], Zhong-Ping Feng [a,b,†], Lingyun Zhang [a], Hossein Pajouhesh [a], Xinpo Jiang [a,‡], Adam Hendricson [a,§], Haiheng Dong [a,¶], Elizabeth Tringham [a], Yanbing Ding [a,‖], Todd W. Vanderah [c], Frank Porreca [c], Francesco Belardetti [a], Gerald W. Zamponi [b], Lester A. Mitscher [d], Terrance P. Snutch [e,*]

[a] Zalicus Pharmaceuticals Ltd, 301-2389 Health Sciences Mall, Vancouver, BC, Canada
[b] Department of Physiology and Pharmacology, University of Calgary, Calgary, Alberta, Canada
[c] Department of Pharmacology, University of Arizona, Tucson, Arizona, USA
[d] Department of Medicinal Chemistry, University of Kansas, Lawrence, KS, USA
[e] Michael Smith Laboratories, University of British Columbia, Vancouver, BC, Canada

ABSTRACT

We previously reported the small organic N-type calcium channel blocker NP078585 that while efficacious in animal models for pain, exhibited modest L-type calcium channel selectivity and substantial off-target inhibition against the hERG potassium channel. Structure–activity studies to optimize NP078585 preclinical properties resulted in compound **16**, which maintained high potency for N-type calcium channel blockade, and possessed excellent selectivity over the hERG (~120-fold) and L-type (~3600-fold) channels. Compound **16** shows significant anti-hyperalgesic activity in the spinal nerve ligation model of neuropathic pain and is also efficacious in the rat formalin model of inflammatory pain.

© 2012 Elsevier Ltd. All rights reserved.

Calcium channels are the primary route of translating electrical signals into biochemical events that underlie key processes such as neurotransmitter release, cell excitability and gene expression.[1] Calcium channels are classified into five pharmacological and physiological subtypes: L-, N-, P/Q-, R- and T-types. Among these, the N-, P/Q- and R-type channels have all been shown to play key roles in neurotransmitter release.[2] In particular, N-type calcium channels are located at the presynaptic terminals of a subset of spinal cord neurons where they mediate transmission of pain signals from the periphery to the central nervous system. The block of N-type channels with peptide agents has been shown to play a significant role in the pathophysiological processes of inflammatory and neuropathic pain.[3]
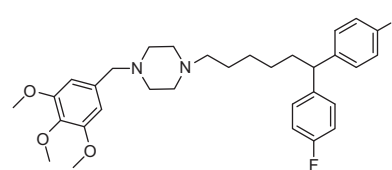

Figure 1. Chemical structure of NP078585.

Previously, we have reported NP078585 (Fig. 1) as an N-type calcium channel blocker with good in vivo efficacy in the rat formalin model of inflammatory pain following oral administration.[4] NP078585 is a potent (IC$_{50}$ = 0.11 μM) and CNS penetrant N-type channel blocker with moderate selectivity over the L-type calcium channel (IC$_{50}$ = 2.8 μM). A potential development concern is that NP078585 also blocked the hERG potassium channel (IC$_{50}$ = 0.4 μM).

In order to further optimize the development of orally available N-type blockers, a major goal was to minimize hERG channel inhibition compared to NP078585. In this regard, in the current study we assessed; (i) modification of aryl substituents on the benzyl moiety bound to the piperazine core of NP078585, (ii) conversion of amines to amides, (iii) aliphatic substitutions on the piperazine

---

* Corresponding author. Tel.: +1 604 822 6968; fax: +1 604 822 6470.
E-mail address: snutch@msl.ubc.ca (T.P. Snutch).
† Present address: Department of Physiology and Biophysics, University of Toronto, Toronto, Ontario, Canada.
‡ Present address: Genscript Technology Co., Ltd, 78 Shuangbaixiang, Xiaolingwei, Xuanwu, Nanjing, Jiangsu, China.
§ Present address: Bristol-Myers Squibb, 345 Park Avenue, New York, USA.
¶ Present address: WuXi AppTec Co. Ltd, 288 Fute Zhong Road, Shanghai, China.
‖ Present address: Shanghai Chempartner Co. Ltd, Pudong New Area, Shanghai, China.
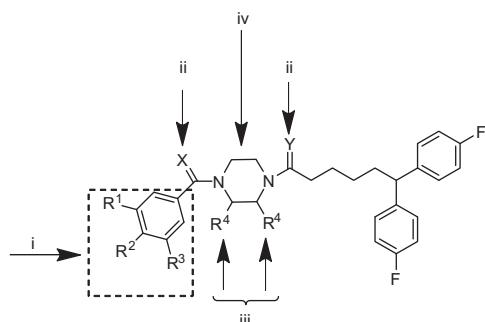
Figure 2. SAR studies focused on: (i) modification of R^1. R^2 and R^3 substituents, (ii) changing the amine into amide, (iii) aliphatic substitution on the piperazine core, and (iv) replacement of piperiazine core with 3-aminomethyl-pyrrolidine.

core, and (iv) replacement of the piperazine core with 3-amino-methyl-pyrrolidine (Fig. 2).

Structure–activity relationship studies initially examined a range of alternative substitution at the trimethoxybenzyl portion of NP078585 with the aim of identifying a series with improved in vitro channel selectivity profiles and with a reduction of hERG inhibition. Compounds **1–14** were prepared from intermediates A and B according to the general synthesis[5] outlined in Scheme 1.

The structure–activity studies of this chemical series were guided by a whole cell manual patch clamp electrophysiology assay for the N-type and L-type calcium channel with further assessment for hERG activity.[6] The replacement of R^1 and R^3 groups on the benzyl region of parent compound NP078585 with a *t*-butyl group (Table 1), in general resulted in maintaining good N-type channel blocking affinity for most compounds. This region of the molecule appears to be fairly accommodating, accepting a *t*-butyl group in 3 and 5 positions being the most optimal substituents, such as compounds **3–12**, all of which showed better or similar

N-type affinities compared to the parent compound NP078585. The 3,5-di-*t*-butyl analogs (compounds **11–12**) also maintained high affinity N-type inhibition with IC$_{50}$ values of 0.14–0.3 μM. Compared to NP078585, the addition of a 4-methoxy substituent (compound **10**) slightly improved affinity ($\sim$0.09 μM) and additionally dramatically improved selectivity both over the L-type channel to greater than 900-fold (IC$_{50}$ $\sim$81 μM, not shown) and the hERG channel by approximately 100-fold (IC$_{50}$ $\sim$9 μM). From this initial series, we determined that 3,5-substitution of the phenyl ring was preferred. Further, the incorporation of a hydrogen bond acceptor (–OCH$_3$) as in the case of compound **10** increased the selectivity for the N-type over the L-type and hERG targets. In general, the amine-linked analogues exhibited higher affinity for hERG as compared to the amide counterparts.

Using aryl substituents (R^1 = *t*-butyl, R^2 = OCH$_3$, R^3 = *t*-butyl) and an amide-linked functional group, we further explored substitutions off the piperazine ring with aliphatic groups. Table 2 shows that *S*-Me substitution was tolerated off the piperazine ring adjacent to the linker (compound **15**) although resulted in high affinity hERG channel blockade (IC$_{50}$ $\sim$0.9 μM). Contrastingly, *S*-Me substitution adjacent to the benzoyl linker (compound **16**) resulted in excellent N-type channel blockade and approximately 3600-fold selectivity over the L-type channel. In addition, compound **16** maintained the favorable hERG channel block of the parent compound **10** (IC$_{50}$ = 4.9 μM). Due to its combined N-type affinity and excellent selectivity profile compound **16** was progressed into in vivo anti-nociception assessment.

Further optimization of NP078585 was attempted by replacement of the piperazine core with 3-aminomethyl-pyrrolidine. We hypothesized that 3-aminomethyl-pyrrolidine could be a potential bioisostere for the piperazine core due to the relatively planar conformation of the pyrrolidine ring in combination with the flexible 3-aminomethyl group. To test this, we synthesized a series of compounds containing amine and amide groups, in combination with a
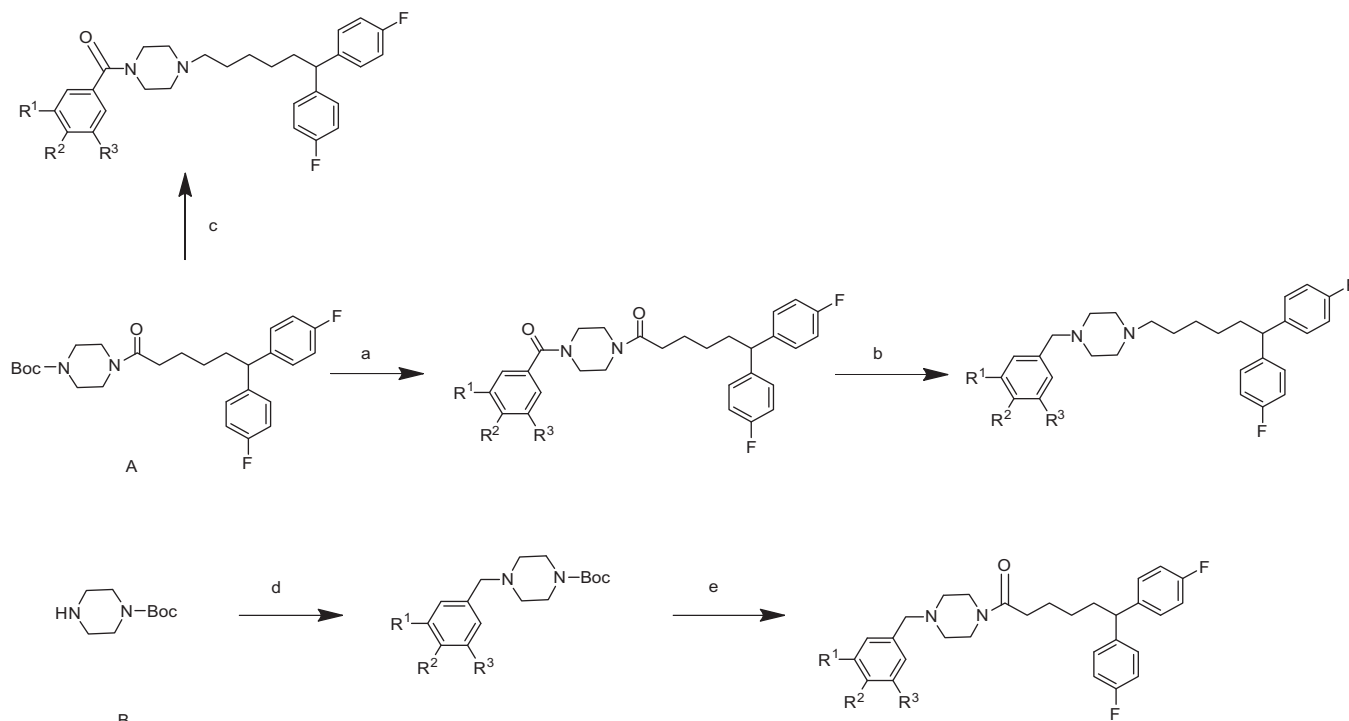
Scheme 1. Reagents and conditions: (a) (i) TFA, CH$_2$Cl$_2$, (ii) benzoic acid analogs, EDC, DMAP, CH$_2$Cl$_2$; (b) LiAlH$_4$, THF; (c) (i) LiAlH$_4$, THF, (ii) TFA, CH$_2$Cl$_2$, (iii) benzoic acid analogs, EDC, DMAP, CH$_2$Cl$_2$; (d) (i) benzoic acid analogs, EDC, DMAP,CH$_2$Cl$_2$, (ii) LiAlH$_4$, THF; (e) (i) TFA, CH$_2$Cl$_2$, (ii) 6,6-bis(4-fluorophenyl)hexanoic acid, EDC, DMAP, CH$_2$Cl$_2$.

Table 1
Blocking activities of compounds **1–14** against the N-type calcium channel and the hERG potassium channel
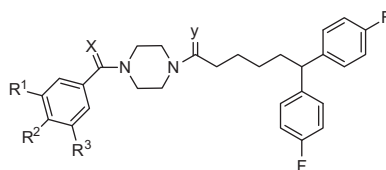
Compound	R^1	R^2	R^3	X	Y	N-type Est. IC_{50} (μM)	hERG Est. IC_{50} (μM)
NP078585	OCH_3	OCH_3	OCH_3	H	H	0.11 (±0.03)	0.4
1	OCH_3	OH	OCH_3	H	H	0.4 (±0.2)	ND
2	OCH_3	OH	OCH_3	O	O	0.6 (±0.39)	ND
3	*t*-Butyl	OH	*t*-Butyl	H	H	0.04 (±0.03)	0.1
4	*t*-Butyl	OH	*t*-Butyl	O	H	0.15 (±0.08)	0.25
5	*t*-Butyl	OH	*t*-Butyl	H	O	0.18 (±0.12)	ND
6	*t*-Butyl	OH	*t*-Butyl	O	O	0.22 (±0.11)	ND
7	*t*-Butyl	OCH_3	*t*-Butyl	H	H	0.09 (0.04)	0.1
8	*t*-Butyl	OCH_3	*t*-Butyl	O	H	0.11 (±0.02)	0.66
9	*t*-Butyl	OCH_3	*t*-Butyl	H	O	0.1 (±0.03)	0.13
10	*t*-Butyl	OCH_3	*t*-Butyl	O	O	0.09 (±0.05)	9.0
11	*t*-Butyl	H	*t*-Butyl	H	H	0.14 (±0.08)	0.1
12	*t*-Butyl	H	*t*-Butyl	O	O	0.3 (±0.25)	ND
13	CF_3	H	CF_3	H	H	1.1 (±1)	ND
14	CF_3	H	CF_3	O	O	0.51(±0.28)	ND

Table 2
Blocking activities of compounds **15–16**

Compound	Structure	N-type Est. IC_{50} (μM)	L-type Est. IC_{50} (μM)	hERG Est. IC_{50} (μM)
15		0.01 (*n* = 2)	ND	0.9
16		0.04 (±0.03)	144	4.9

3-aminomethyl-pyrrolidine scaffold with known structural elements of NP078585 and compound **10**.

Initial efforts in this study focused on analogs wherein substitutions on the aryl group were varied (Table 3). The synthesis of these compounds is as described in Scheme 2 and is illustrative of the general procedure. Briefly, readily available 1-benzyl-pyrrolidin-3-ylmethyl- carbamic acid tert-butyl ester was debenzylated via catalytic hydrogenation followed by coupling with 6,6-bis(4-fluorophenyl)hexanoic acid mediated by EDC and DMAP to provide the desired intermediate. Subsequent deprotection of the Boc group and reaction with the appropriate benzoic acid provided desired compounds. Reduction of the di-amide moiety with LiAlH$_4$ proceeded smoothly to afford di-amines compounds.[7]

Compounds (**17–28**) generally exhibited highly favorable N-type channel inhibition (IC$_{50}$ values ~0.04–0.9 μM). Of these, compounds **18–19** and **26–27** containing bulky substituents (*t*-butyl) on the 3,5-position of the aryl group showed improved N-type channel inhibition compared to NP078585. Of note, compound **19** with the highest N-type affinity also showed excellent selectivity over the L-type calcium channel (~750-fold; not shown). Extending the substitution of the phenyl ring to trifluoromethyl (compounds
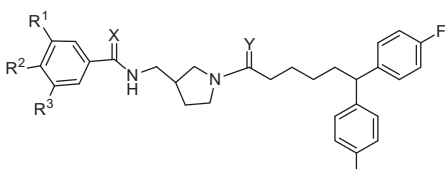
20–21) did not improve activity concerning N-type blockade and further, the best of these (compound **20**, IC$_{50}$ ~0.2 μM) exhibited a poor hERG profile. Comparing amine-linked compounds **23–27** to their amide counterparts (compounds **17–21**), in general the di-amine linked analogues possessed higher affinity for both the N-type calcium channel and the hERG potassium channel as compared to their di-amide counterparts.

The stereogenic center introduced by the pyrrolidine ring appeared to have little effect on N-type calcium channel activity with the *R:S* IC$_{50}$ values approaching unity (Table 4). These observations would seem to be one of the many exceptions to Pfeiffer's rule, which states that the higher the activity of a eutomer, the higher the separation in activities between eutomer and distomer.[8]

We further then focused on understanding the effect of replacing one phenyl group on the benzhydryl with piperidine (Scheme 3). The introduction of the N-piperidinyl moiety (compounds **35–37**) resulted in analogs with reduced N-type affinity relative to the corresponding phenyl analogs (see Table 5).

Based on the encouraging results associated with compound **19**, we investigated whether swapping the 'left hand' and 'right hand' side moieties attached to the 3-amino(methyl) pyrrolidine core

Table 3
Blocking activities of compounds 17–27 against the N-type calcium channel and the hERG potassium channel

Compound	R^1	R^2	R^3	X	Y	N-type Est. IC$_{50}$ (μM)	hERG Est. IC$_{50}$ (μM)
17	H	t-Butyl	H	O	O	0.08 (±0.04)	0.82
18	t-Butyl	H	t-Butyl	O	O	0.11 (±0.06)	2.8
19	t-Butyl	OCH$_3$	t-Butyl	O	O	0.04 (n = 2)	1.9
20	CF$_3$	H	CF$_3$	O	O	0.21 (±0.15)	0.7
21	CF$_3$	H	F	O	O	0.75 (±1.24)	ND
22	t-Butyl	OCH$_3$	t-Butyl	O	H	0.09 (n = 2)	0.1
23	OCH$_3$	OCH$_3$	OCH$_3$	O	H	0.28 (±0.18)	0.1
24	CF$_3$	H	CF$_3$	O	H	0.15 (n = 2)	0.1
25	OCH$_3$	OCH$_3$	OCH$_3$	H	H	0.06 (±0.04)	0.04
26	t-Butyl	OH	t-Butyl	H	H	0.05 (±0.03)	0.87
27	t-Butyl	H	t-Butyl	H	H	0.03 (n = 2)	0.46
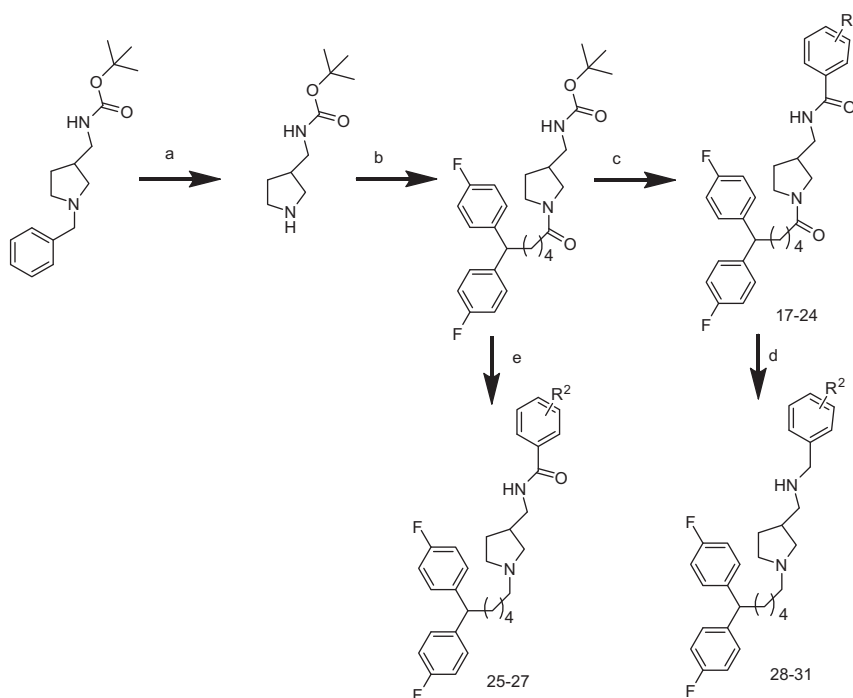
Scheme 2. Reagents and conditions: (a) Pd/C, H$_2$, MeOH; (b) 6,6-bis(4-fluorophenyl)hexanoic acid or 6-(1-methylpiperidin-4-yl)-6-phenylhexanoic acid, EDC, DMAP, CH$_2$Cl$_2$; (c) (i) TFA, CH$_2$Cl$_2$, (ii) benzoic acid analogs, EDC, DMAP, CH$_2$Cl$_2$; (d) LiAlH$_4$·THF; (e) (i) LiAlH$_4$·THF, (ii) TFA, CH$_2$Cl$_2$, (iii) benzoic acid analogs, EDC, DMAP, CH$_2$Cl$_2$.
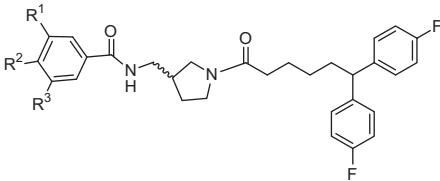
(Table 6). The change proved to be well tolerated and yielded one analogue with excellent affinity for N-type calcium channel (compound 39, IC$_{50}$ ∼0.01 μM). Unfortunately, these modifications did not offer any advantages concerning hERG selectivity over compound 20.

Of the compounds synthesized and evaluated, compounds 10 and 16 exhibited the most promising overall in vitro target profiles; N-type blocking IC$_{50}$s ∼0.04–0.09 uM and excellent selectivity over both the L-type calcium channel (∼900- to 3600-fold) and hERG potassium channel (∼ 100- to 122-fold). Reflective of these combined properties, compounds 10 and 16 were selected for in vivo assessment in the rat formalin model of inflammatory pain.[9] Upon intraperitoneal (ip) administration only compound

16 exhibited significant antinociceptive activity (∼50–60% of vehicle-treated group) in phase II and phase IIA of the formalin response (Table 7).

Compounds 10 and 16 were also evaluated for activity in the Chung model of neuropathic pain[10] with two behavioral endpoints used: mechanical allodynia[11] and thermal hyperalgesia.[12] Animals were administered a single 30 mg/kg oral dose of each compound and were tested at 30 min intervals during a 2–3 h test period beginning 30 min after test compound administration. One-way ANOVA followed by the Bonferroni test were employed on the original raw data (not normalized) to establish the statistical significance of the differences observed with the post SNL-baseline value. Compounds 10 and 16 both demonstrated efficacious

Table 4
The effect of chirality for compounds **28–33** on the N-type and hERG blocking activities

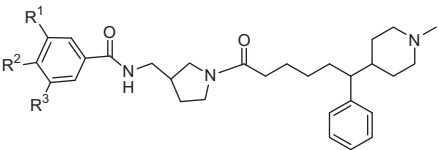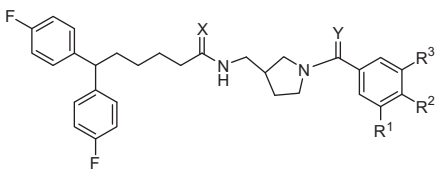| Compound	Stereochemistry	R^1	R^2	R^3	N-type Est. IC$_{50}$ (µM)	hERG Est. IC$_{50}$ (µM)
28	R	t-Butyl	H	t-Butyl	0.16 (±0.18)	5.0
29	S	t-Butyl	H	t-Butyl	0.12 (±0.03)	2.0
30	R	t-Butyl	OCH$_3$	t-Butyl	0.15 (±0.02)	5.0
31	S	t-Butyl	OCH$_3$	t-Butyl	0.36 (±0.2)	2.0
32	R	CF$_3$	H	CF$_3$	0.1 (±0.02)	0.75
33	S	CF$_3$	H	CF$_3$	0.09 (±0.03)	0.8
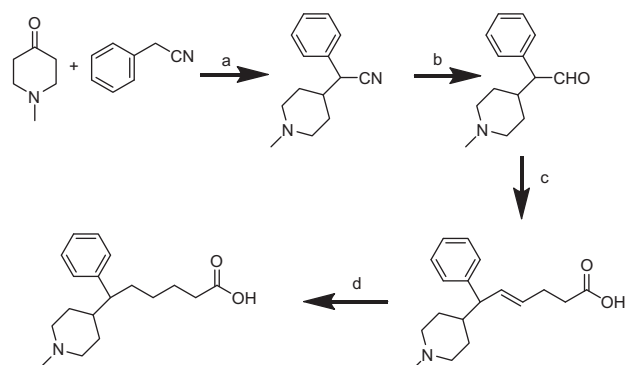
Scheme 3. Reagents and conditions: (a) NaOMe, MeOH; (b) Dibal, CH$_2$Cl$_2$; (c) LiHMDS, THF; (d) Pd/C, H$_2$, 50 Psi, MeOH.

Table 5
N-type calcium channel blocking activities for compounds **34–37**

Compound	R^1	R^2	R^3	N-type Est. IC$_{50}$ (µM)
34	OCH$_3$	OCH$_3$	OCH$_3$	3.2 (±2.8)
35	Isopropyl	OCH$_3$	Isopropyl	1.9 (±2.2)
36	CH$_3$	OCH$_3$	CH$_3$	0.1 (±0.02)
37	Cl	H	Cl	0.88 (±0.33)

Table 6
N-type calcium channel and hERG potassium channel blocking activities for compounds **38–42**

Compound	R^1	R^2	R^3	X	Y	N-type Est. IC$_{50}$ (µM)	hERG Est. IC$_{50}$ (µM)
38	OCH$_3$	OCH$_3$	OCH$_3$	O	O	0.84 (±0.39)	0.75
39	t-Butyl	OCH$_3$	t-Butyl	O	O	1.9 (±2.2)	0.65
40	OCH$_3$	OCH$_3$	OCH$_3$	H	H	0.06 (±0.06)	0.1
41	t-Butyl	OH	t-Butyl	H	H	0.004 (n = 2)	0.01
42	t-Butyl	OCH$_3$	t-Butyl	H	H	0.032	0.11

Table 7
Efficacy of compounds **10** and **16** in the rat formalin model of acute inflammatory pain

Compound	% Of vehicle response		
	Phase I	Phase II	Phase IIA
10	79 ± 6	80 ± 7	67 ± 5
16	79 ± 9	61 ± 9***	50 ± 12**

Compounds, prepared in propylene glycol, were administered at a dose of 30 mg/kg ip at 3 mL/kg 30 min prior to intraplantar injection of formalin into the hindpaw. Data are the mean percent of vehicle effect (MPE) ± SEM, $n = 5$ animals tested for compound **10** and $n = 6$ animals for compound **16**. Data were analyzed for significance using a one-way ANOVA to vehicle-treated group. **$P <0.01$; ***$P <0.001$

inhibition of nerve ligation-induced thermal hyperalgesia (ranging from ~54% to 86% maximal antinociception; Table 8). Contrastingly, only compound **16** exhibited discernible antiallodynic effects in vivo. This may reflect distinct underlying pathophysiological mechanisms contributing to these two pain behavioral endpoints together with any as yet-to-be determined unique state-dependent target and/or off-target activities related to compounds **10** and **16**.

In summary, we have described a series of piperazine and 3-amino(methyl)pyrrolidine analogues, some of which display both excellent potency as N-type calcium channel antagonists and possess favorable selectivity over the hERG potassium channel. Among these, compound **16** exhibited good selectivity over the L-type calcium channel and showed analgesic activity in both inflammatory and neuropathic rat pain models. The development of N-type calcium channel blockers for eventual clinical usage will require optimization of multiple parameters, including high affinity and selectivity for the N-type target, suitable pharmacokinetic charac-

Table 8
Efficacy in the neuropathic SNL rat model for compounds **10** and **16**

Compound	Tactile allodynia: maximum % antinociception at 60 min	Thermal hyperalgesia: maximum % antinociception at 60 min
10	1.9 ± 1.4	54.2 ± 12.9**
16	31.7 ± 6.9**	85.8 ± 14.1**

Compounds, prepared in propylene glycol, were administered at a dose of 30 mg/kg po at 1 mL/kg after baseline assessment for neuropathic pain and behavioral assessments were performed at 30 min intervals post-administration, up to 3 h. Data are the mean percent of maximal possible antinociception ± SEM; n = 5–6 animals. The following formula was used to calculate the % anti-allodynic activity: $100\% \times$ [(paw withdrawal thresholds after drug treatment – postSNL baseline paw withdrawal thresholds)/ (preSNL baseline paw withdrawal thresholds – postSNL baseline paw withdrawal thresholds). The following formula was used to calculate the % anti-hyperalgesic activity: $100\% \times$ [(paw withdrawal latencies after drug treatment – postSNL baseline paw withdrawal latencies)/(preSNL baseline paw withdrawal latencies – postSNL baseline paw withdrawal latencies). Data from the ipsilateral paw were also assessed by a one-way ANOVA-post-hoc for statistical significance. **P <0.01.

teristics incorporating oral bioavailability and blood–brain barrier penetration, and a wide therapeutic index against the cardiovascular, nervous and other systems. Similar to our previous reports,[4,13] only a subset of high affinity in vitro N-type channel blockers in the current study exhibited efficacy in rodent neuropathic and inflammatory pain models. An exact correlation between in vitro target affinity and in vivo analgesia is generally lacking across many similar studies, making direct compound-based predictive assessments difficult and requiring empirical elucidation of efficacy. In part, this may reflect a requirement for an optimal combination of high affinity N-type channel blockade acting via a state- and/ or frequency-dependence mechanism and reflective of the underlying pathophysiology associated with specific pain states.[14]

Acknowledgements

References and notes

1. (a) Barclay, J. W.; Morgan, A.; Burgoyne, R. D. *Cell Calcium* **2005**, *38*, 343; (b) Zheng, X.; Bobich, J. A. *Brain Res. Bull.* **1998**, *47*, 117.
2. (a) Bowersox, S. S.; Valentino, K. L.; Luther, R. R. *Drug News Perspect.* **1994**, *7*, 261; (b) Bean, B. P. *Annu. Rev. Physiol.* **1989**, *51*, 367; (c) Hess, P. *Annu. Rev. Neurosci.* **1990**, *13*, 337; (d) Nooney, J. M.; Lambert, R. C.; Feltz, A. *Trends Pharmacol. Sci.* **1997**, *18*, 363.
3. (a) Sheng, Z. H.; Rettig, J.; Cook, T.; Catterall, W. A. *Nature* **1996**, *379*, 451; (b) Saegusa, H.; Kurihara, T.; Zong, S.; Kazuno, A.; Matsuda, Y.; Nonaka, T.; Han, W.; Toriyama, H.; Tanabe, T. *EMBO J.* **2001**, *20*, 2349; (c) Cox, B.; Denyer, J. C. *Expert Opin. Ther. Patents* **1998**, *8*, 1237.
4. Zamponi, G. W.; Feng, Z. P.; Zhang, L.; Pajouhesh, Ho.; Ding, Y.; Belardetti, F.; Pajouhesh, Ha.; Dolphin, D.; Mitscher, L. A.; Snutch, T. P. *Bioorg. Med. Chem. Lett.* **2009**, *19*, 6467.
5. Pajouhesh, Ho.; Zamponi, G. W.; Pajouhesh, Ha..; Belardetti, F.; Snutch, T. P. *WO* 2004/089922 and *U.S. Patent* 2004/0044004 A1.
6. The structure–activity analyses of the various chemical series were guided by manual whole-cell patch clamp electrophysiological assay of rat neuronal N-type (Bourinet, E.; Soong, T.-W.; Sutton, K.; Slaymaker, S.; Mathews, E.; Monteil, A.; Zamponi, G. W.; Nargeot, J.; Snutch, T. P. *Nat. Neurosci.* **1999**, *2*, 407) and L-type (Snutch, T. P.; Tomlinson, W. J.; Leonard, J. P.; Gilbert, M. M. *Neuron* **1991**, *7*, 45) channels transiently expressed in HEK293 cells (N-type: α_{1B}/Ca$_V$2.2 + $\alpha_2\delta$-1 + β_{1b} subunits; L-type: α_{1C}/Ca$_V$1.2 + $\alpha_2\delta$-1 + β_{1b} subunits). Compounds were also assayed against the hERG potassium channel stably expressed in HEK293 cells. Whole cell barium currents were elicited from a holding potential of −100 mV to the peak of current–voltage relation for each channel type. With a few exceptions, each compound was examined for blockade on 3–5 cells. Testing compounds for blockade of N-type and L-type calcium channels was performed by whole-cell manual patch clamp analysis using a near half-maximal concentration of compound applied to HEK293 cells as per Ref.[4]. Pipettes (in the range of 2–4 MΩ) were filled with an internal solution containing 108 mM Cs-methanesulfonate, 4 mM MgCl$_2$, 9 mM EGTA, 9 mM HEPES (pH 7.2 adjusted with TEA-OH) for N- and L-type channel currents and 130 KCl, 1 MgCl$_2$, 5 EGTA, 10 HEPES, 5 K$_2$ATP (pH 7.2 with KOH) for hERG K$^+$ channel currents. Whole-cell barium currents were recorded using an Axopatch 200B amplifier and an extracellular recording solution comprised of 5 mM BaCl$_2$, 1 mM MgCl$_2$, 10 mM HEPES, 40 mM TEA-Cl, 10 mM glucose, 97.5 mM CsCl (pH 7.2 adjusted with TEA-OH) for N- and L-type channel currents and 137 NaCl, 4 KCl, 1.8 CaCl, 1 MgCl$_2$, 10 HEPES, 10 glucose (pH 7.4 with NaOH) for hERG K$^+$ channel currents. Data were filtered at 1 kHz using a four pole Bessel filter and digitized at a sampling frequency of 2 kHz. Whole-cell barium current inhibition was measured from a holding potential of −80 mV to a test potential of +10 mV, applied at 0.2 Hz, or from a holding potential of −80 mV to +1-mV following a 1 s prepulse to −60 mV, applied at 0.067 Hz for N-type channels. L-type channel currents were obtained from a holding potential of −80 mV to a test potential of +10 mV, applied at 0.2 Hz. To study compound effects on the hERG channel using manual patch clamp, the peak of the slowly deactivating tail current was examined. A 2 s depolarization to +60 mV from a holding potential of −80 mV, followed by a repolarization to −50 mV was used to generate the hERG tail currents.
   The estimated IC$_{50}$ value was then calculated for all compounds tested in the various electrophysiological assays such that estimated IC$_{50}$ = [D]/((1/fr)-1) where [D] is the drug concentration, and fr is the fraction of current remaining after drug application. This analysis assumes that there is a 1:1 interaction between the drug and the channel. The term 'estimated IC$_{50}$ value' is utilized since the determination of IC$_{50}$ value via a single concentration point may be slightly less precise than fits to entire concentration-dependent response curves. For some compounds IC$_{50}$ values were obtained using data obtained from multiple concentrations and fitted with a logistic function where max is the maximum current amplitude in the absence of compound, min is the minimum current amplitude at steady-state inhibition with the compound and n_H is the Hill slope:

$$y = \left[\frac{\max - \min}{1 + \left(\frac{[\text{drug}]}{\text{IC}_{50}} \right)^{n_H}} \right] + \min$$

7. Pajouhesh, Ha.; Snutch, T.P.; Pajouhesh, Ho.; Ding, Y. U.S. Patent 20050014748 A1, 2005.
8. Pfeiffer, C. C. *Science* **1956**, *124*, 29.
9. (a) Dubuisson, D.; Dennis, S. G. *Pain* **1977**, *4*, 161; (b) Malmberg, A. B.; Yaksh, T. L. *J. Neurosci.* **1994**, *14*, 4882.
10. Kim, S. H.; Chung, J. M. *Pain* **1992**, *50*, 355.
11. Chaplan, S. R.; Bach, F. W.; Pogrel, J. W.; Chung, J. M.; Yaksh, T. L. *J. Neurosci. Methods* **1994**, *53*, 55.
12. Hargreaves, K.; Dubner, R.; Brown, F.; Flores, C.; Joris, J. *Pain* **1988**, *32*, 77.
13. Pajouhesh, Ho; Feng, Z.-P.; Ding, Y.; Zhang, L.; Pajouhesh, Ha; Morrison, J.-L.; Belardetti, F.; Tringham, E.; Simonson, E.; Vanderah, T. W.; Porreca, F.; Zamponi, G. W.; Mitscher, L. A.; Snutch, T. P. *Bioorg. Med. Chem. Lett.* **2010**, *20*, 1378.
14. Snutch, T. P. *NeuroRx* **2005**, *2*, 662.